Adaptive Exploration Harmony Search for Effective Parameter Estimation in an Electrochemical Lithium-Ion Battery Model

HUIYONG CHUN[ID]**, MINHO KIM**[ID]**, JUNGSOO KIM**[ID]**, KWANGRAE KIM,
JUNGWOOK YU, TAEGYUN KIM, AND SOOHEE HAN**[ID]

Department of Creative IT Engineering, Pohang University of Science and Technology, Pohang 37673, South Korea

Corresponding author: Soohee Han (soohee.han@postech.ac.kr)

ABSTRACT Electrochemical models of lithium-ion batteries are derived according to the laws of physics; therefore, the parameters represent specific physical quantities such as lithium diffusivities, particle volume fractions, and ion intercalation rates. It is important to estimate these parameters to identify the internal states of a lithium-ion battery for efficient and safe management. Until now, parameter estimation algorithms for electrochemical lithium-ion battery models have been developed without considering the unequal identifiability among the target parameters. Thus, it is highly likely that existing algorithms exhibit inefficient exploration and lead to a slow convergence rate and even large parameter estimation error. For more accurate parameter estimation of an electrochemical lithium-ion battery model, we propose a new adaptive exploration harmony search (AEHS) scheme that provides a wide search space for a longer period of time when estimating parameters with low identifiability. The proposed algorithm is based on improved harmony search; its bandwidth parameters for determining the level of exploration are adjusted according to the individual and joint variabilities computed from the distributions of previously estimated parameters. Such adaptive bandwidth parameters can reduce inefficient exploration and enable fast convergence, allowing exploration that achieves global optimality. Simulation results show that the proposed parameter estimation algorithm produces the highest convergence rate and the smallest parameter estimation error compared with existing schemes. The performance of the proposed scheme is also validated using real data generated from experiments.

INDEX TERMS Adaptive exploration harmony search, electrochemical model, lithium-ion battery, meta-heuristic algorithm, parameter estimation, parameter identifiability.

I. INTRODUCTION

Lithium-ion batteries are a promising energy source as they exhibit higher energy and power density than any other type of energy storage device. However, they suffer from battery life degradation and even safety problems such as ignition and explosion. For efficient and safe management, lithium-ion batteries must be handled carefully with constant observation of their changing internal states. Some of the degradation

The associate editor coordinating the review of this manuscript and approving it for publication was Edith C.-H. Ngai.

mechanisms that occur inside a battery are strongly related to its internal states. For example, the available capacity, power, and energy in a lithium-ion battery is gradually reduced by the accumulation of a solid electrolyte interface (SEI) layer at the anode and undesired by-product at the cathode [1]–[3]. If these degradation mechanisms can be diagnosed over time, it is highly possible to operate lithium-ion batteries efficiently and safely.

Electrochemical models of lithium-ion batteries have been employed to observe their internal physicochemical changes by describing transport and diffusion phenomena at the

micro-scale. As an electrochemical model is built by employing fundamental physical principles, its parameters represent specific physical quantities. For example, aging-relevant parameters in the model, termed aging parameters in this paper, are very helpful for determining the internal state of the lithium-ion battery as their values change consistently with the aging progress. However, it is difficult to estimate these parameters from measured data because the electrochemical lithium-ion battery model consists of several linked partial differential equations (PDEs) over space and time, as well as the required boundary conditions.

Various optimization algorithms have been employed to estimate the parameters of an electrochemical lithium-ion battery model; for example, the Gauss-Newton method, a well-known Jacobian-based algorithm [4]. However, an electrochemical lithium-ion battery model with several PDEs and boundary conditions is highly nonlinear and complicated; therefore, parameter estimation with a Jacobian-based algorithm may fall into a local optimal solution [5]. Besides Jacobian-based algorithms, metaheuristic algorithms such as the genetic algorithm (GA) [6]–[8], particle swarm optimization (PSO) [9], and harmony search (HS) [10], [11] have been used to research the fields of a lithium-ion battery and a fuel cell. Although these metaheuristic algorithms have relatively low convergence rates compared to Jacobian-based algorithms, they are capable of finding the global optimum without becoming stuck in a local optimum. Therefore, metaheuristic algorithms may be more appropriate for parameter estimation of a full order, or non-approximated, electrochemical lithium-ion battery model that may have multiple local optima.

Despite the aforementioned advantage for finding the global optimal solution, existing metaheuristic algorithms have an inherent limitation in that they explore the offline predetermined search space without considering the consistently directional effects of the target parameters when optimizing an objective function. Such a limitation may be significant in the parameter estimation of an electrochemical lithium-ion battery model. The consistently directional effect of the target parameter; i.e., how consistently the parameter converges in a direction towards the global optimum, is called the identifiability. In fact, each target parameter has a different identifiability [7], [12]–[15]; therefore, the search space may be too large or too small if determined equally. As a result, it is more efficient to adaptively determine the search space size according to the identifiability of a parameter. As strongly identifiable parameters tend to converge rapidly towards true values due to their consistently directional effect when optimizing an objective function, it is advantageous to specify a small search space in order to avoid inefficient exploration and ensure a rapid convergence rate. Conversely, weakly identifiable target parameters require a relatively long time to explore true values. Hence, it is advantageous for them to have a large search space for a longer period of time to facilitate finding a better solution. Thus, fast and

accurate parameter estimation requires the development of a metaheuristic algorithm that determines the level of exploration for each target parameter according to its identifiability.

With the goal of more accurate parameter estimation of an electrochemical lithium-ion battery model, we develop a novel metaheuristic algorithm based on HS, which effectively determines the search space size by considering parameter identifiability. The adopted HS is generally acknowledged to have a faster convergence rate than other metaheuristic algorithms such as GA and PSO because it does not handle many candidate parameter sets [16]–[19]. In the same way musicians may search for a perfect harmony by improvising pitches using their memories, HS seeks an optimal solution through a potential combination of components of all available candidate parameter sets in its memory [16]. This differs to GA, which generates new solution vectors from only two of the existing vectors, called parents. Thus, HS generates widely explored parameter sets despite the small number of candidate parameter sets in its memory and exhibits a fast convergence rate [20]. In summary, HS has strong exploration ability with an easily implemented simple structure.

This study proposes a novel HS-based parameter estimation scheme, called adaptive exploration harmony search (AEHS), to provide effective exploration by considering the unequal identifiability among the parameters to be estimated. For more accurate estimation of electrochemical lithium-ion battery models, parameters with low identifiability are explored in a wide search space for a longer period of time than those with relatively high identifiability. To this end, the matrix, called the past best memory (PBM), is constructed as a superset of the existing harmony memory (HM), which stores a given number of the superior candidate parameter sets generated up to the current iteration. The proposed AEHS scheme computes the variability of each parameter in the PBM then provides a wider search space when estimating parameters with large variability or low identifiability. Specially, the bandwidth parameters of HS employed for the proposed AEHS scheme are adjusted to determine the level of exploration by computing the individual and joint variabilities from the distributions of previously estimated parameters. Such adaptive bandwidth parameters can reduce inefficient exploration for more rapid convergence and enable exploration that achieves global optimality. Moreover, we perform simulations and use real data generated from experiments to validate the performance of the proposed scheme.

This paper is organized as follows: Section 2 describes the electrochemical lithium-ion battery model and introduces the target aging parameters to be estimated. In Section 3, a detailed description of the proposed AEHS scheme is provided together with a brief introduction to HS. Section 4 presents the validation results of our proposed AEHS using both simulations and real data. The conclusions are presented in Section 5.
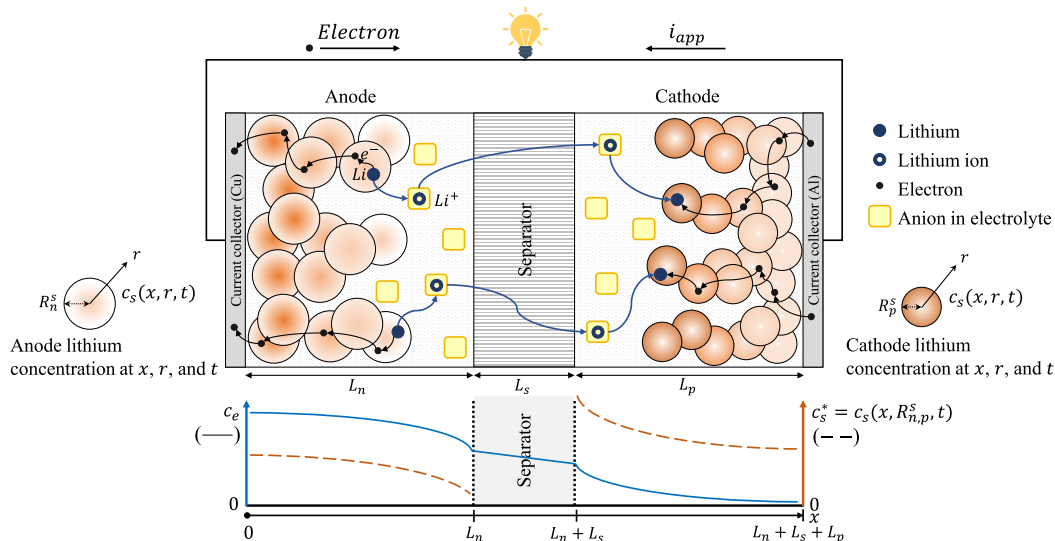
FIGURE 1. Electrochemical reactions inside a lithium-ion battery during the charging process, showing lithium-ion concentration over pseudo two-dimensional space (*x*, *r*) at a certain time, *t*.

II. ELECTROCHEMICAL MODEL AND PARAMETER DESCRIPTION

A. PSEUDO TWO-DIMENSIONAL MODEL

The electrochemical lithium-ion battery model is a systematic and realistic model for representing the internal states of a lithium-ion battery, as shown in Fig. 1, because it is derived from physical phenomena such as the transport and diffusion of charges and lithium-ions.

We employ a continuum model obtained by the volume averaging method as a practical electrochemical model because a micro-scale model is hard to handle [21]. To reduce the computational burden, a pseudo two-dimensional (P2D) model is often adopted by reducing the dimensions of the continuum model by only considering the *x*-axis (lithium-ion flow direction) and pseudo *r*-axis (radial direction in solid particles). Because model reduction is implemented while preserving the electrochemical properties of the lithium-ion battery, the P2D model has been widely used in battery simulations. As seen in Table 1 and 2, this model consists of five governing equations with dozens of parameters; i.e. charge and mass (lithium) conservation in solid particles, charge and mass (lithium) conservation in the electrolyte, and the rate of lithium intercalation at the interface of the particles and electrolyte [22], [23]. A thermal model is included in the simulation to improve the model accuracy because temperature changes may affect some parameter values. Additionally, the model for SEI layer formation which is directly relative to aging phenomena, is combined with the existing model in order to handle the aging information inside the batteries [24].

B. TARGET PARAMETER SELECTION

As mentioned earlier, the P2D model contains dozens of parameters that represent specific physical quantities. As the internal dynamics of the lithium-ion battery vary with the

aging progress, the parameter values also change according to continual aging mechanisms. For example, the porosity; i.e. the volume fraction of the electrolyte, decreases gradually with battery usage because the electrolyte material is reduced by growth of the SEI layer on the solid particles [25]–[27]. As well as porosity, the solid particle diffusivity and reaction rate exhibit a regular decrease with time [4], [9]. It is very important to estimate the aging parameters that are highly affected by degradation mechanisms; thus, we estimate the following eight parameters: three porosities (cathode, anode, separator), two reaction rates (cathode, anode), two solid particle diffusivities (cathode, anode), and resistance of SEI layer. The target parameters to be estimated are denoted by X as follows:

$$X = [\epsilon_p, \epsilon_s, \epsilon_n, D_p^s, D_n^s, k_p, k_n, R_{SEI}]. \quad (1)$$

where all parameters are defined in Table 2.

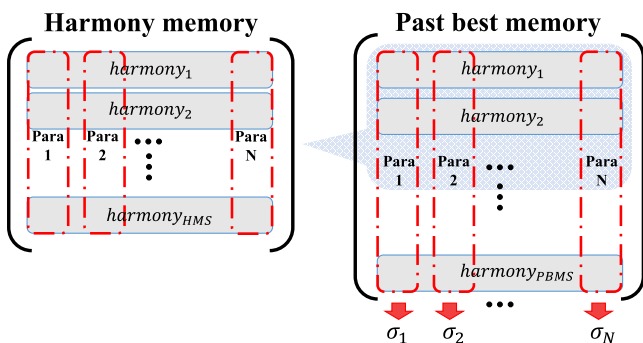## III. ADAPTIVE EXPLORATION HARMONY SEARCH

A. BASIC HARMONY SEARCH

HS has been widely employed in energy related fields such as battery or energy storage system (ESS) due to its superior performance [10], [11], [16], [17], [20], [28], [29]. Basic HS was inspired by the improvisation of musical harmony, which is a combination of sounds [16]. In the same way that musicians seek the optimal harmony from an aesthetic perspective, HS finds an optimal solution determined from an objective function evaluation. The improvisation process is a key idea of HS, and HS imitates the process for the heuristic optimization.

HS uses a memory called harmony memory (HM). Each row of the HM represents one harmony, which is a candidate parameter set for the globally optimal solution, and each column of the HM represents values of the pitch, or a parameter,

TABLE 1. Governing equations and boundary conditions for electrochemical, thermal, and SEI layer formation lithium battery models.

Electrochemical (P2D) model	
Charge conservation in solid particles: $\frac{\partial}{\partial x}(\sigma_{eff}^s \frac{\partial \phi_s}{\partial x}) = a_s F j$	Boundary conditions: $\frac{\partial \phi_s}{\partial x}\|_{x=L_n} = 0 \qquad \frac{\partial \phi_s}{\partial x}\|_{x=L_n+L_s} = 0$ $\frac{\partial \phi_s}{\partial x}\|_{x=L_n+L_s+L_p} = \frac{-i_{app}}{A\sigma_{eff}^s} \qquad \frac{\partial \phi_s}{\partial x}\|_{x=0} = \frac{-i_{app}}{A\sigma_{eff}^s}$
Mass conservation in solid particles: $\frac{\partial c_s}{\partial t} = \frac{1}{r^2}\frac{\partial}{\partial r}(D_{eff}^s r^2 \frac{\partial c_s}{\partial r})$ $\star D_{eff}^s$ depends on $D_{p,n}^s$.	Boundary conditions: $D_{eff}^s \frac{\partial c_s}{\partial r}\|_{r=R_{p,n}^s} = -j \qquad \frac{\partial c_s}{\partial r}\|_{r=0} = 0$
Charge conservation in electrolyte: $\frac{\partial}{\partial x}(\sigma_{eff}^s \frac{\partial \phi_s}{\partial x}) + \frac{\partial}{\partial x}(\kappa_{eff}^e \frac{\partial \phi_e}{\partial x}) + \frac{\partial}{\partial x}(\kappa_D \frac{\partial \ln c_e}{\partial x}) = 0$	Boundary conditions: $\kappa_{eff}^e \frac{\partial \phi_e}{\partial x} + \kappa_D \frac{\partial \ln c_e}{\partial x}\|_{x=0} = \kappa_{eff}^e \frac{\partial \phi_e}{\partial x} + \kappa_D \frac{\partial \ln c_e}{\partial x}\|_{x=L_n+L_s+L_p} = 0$ $\kappa_{eff}^e \frac{\partial \phi_e}{\partial x} + \kappa_D \frac{\partial \ln c_e}{\partial x}\|_{x=L_n} = \kappa_{eff}^e \frac{\partial \phi_e}{\partial x} + \kappa_D \frac{\partial \ln c_e}{\partial x}\|_{x=L_n+L_s} = \frac{-i_{app}}{A}$
Mass conservation in electrolyte: $\epsilon_{p,n}\frac{\partial c_e}{\partial t} = \frac{\partial}{\partial x}(D_{eff}^e \frac{\partial c_e}{\partial x}) + a_s(1-t_+)j$ $\epsilon_s\frac{\partial c_e}{\partial t} = \frac{\partial}{\partial x}(D_{eff}^e \frac{\partial c_e}{\partial x})$	Boundary conditions: $\frac{\partial c_e}{\partial x}\|_{x=0} = \frac{\partial c_e}{\partial x}\|_{x=L_n+L_s+L_p} = 0$
Lithium movement between solid particle and electrolyte: $j = \frac{k_{p,n}\sqrt{c_e(c_s^{max}-c_s^*)c_s^*}}{F}\{exp(\frac{(1-\alpha)F}{RT}\eta) - exp(-\frac{\alpha F}{RT}\eta)\}$	
Thermal dynamic model	
Thermal capacity & generation: $\rho_{p,n}C_p\frac{\partial T}{\partial t} = \frac{\partial}{\partial x}(\lambda_{p,n}\frac{\partial T}{\partial x}) + Q_{ohm} + Q_{rxn} + Q_{rev}$	Boundary conditions: $\lambda_{Cu}\frac{\partial T}{\partial x}\|_{x=0^-} = \lambda_p\frac{\partial T}{\partial x}\|_{x=0^+}$ $\lambda_n\frac{\partial T}{\partial x}\|_{x=L_n+L_s+L_p+0^-} = \lambda_{Al}\frac{\partial T}{\partial x}\|_{x=L_n+L_s+L_p+0^+}$
Solid particle electrolyte interface (SEI) layer dynamic model	
Overpotential in negative electrode: $\eta_n = \phi_s - \phi_e - U_{ref} - \frac{j}{a_n^s}R_{film}$	film resistance: $R_{film} = R_{SEI} + \frac{\delta_{film}}{\kappa_{SEI}}$

FIGURE 2. Structure of the HM and its superset, PBM.

of the harmonies (Fig. 2). The number of rows in the HM is called the harmony memory size (HMS), which represents the number of harmonies stored in the HM. Prior to improvisation, the HM is initialized using randomly generated values between the upper and lower bounds of the pitches. Then, a new harmony, or new candidate parameter set, is generated

from the HM according to the HS design parameters: harmony memory considering rate (HMCR), pitch adjustment rate (PAR), and bandwidth. The range of the adjustment for new harmony's variation is randomly determined from the following bandwidth parameters:

$$\hat{X}_i^{new}(itr) = \check{X}_i(itr) + \theta_i(itr) \cdot bw_i(itr). \qquad (2)$$

where $\theta_i(itr)$ is independently identically distributed (i.i.d.) over the iteration and uniformly distributed over the interval [0,1], $\hat{X}_i^{new}(itr)$ is the i-th pitch, or parameter of the new harmony generated in the itr-th iteration, $\check{X}_i(itr)$ is the i-th pitch that remains according to the HMCR probability, and $bw_i(itr)$ is the value of the i-th bandwidth corresponding to the i-th pitch.

B. PARAMETER IDENTIFIABILITY
Each pitch of the harmony, which represents a target parameter to be estimated, has a different effect on the objective function. A strongly identifiable parameter has a consistently directional effect on optimizing the objective function, and its

TABLE 2. List of parameter symbols and descriptions in the P2D model.

Symbol	Description
ϕ_s	Solid particle potential
ϕ_e	Electrolyte potential
σ_{eff}^s	Effective solid particle conductivity
$L_{p,s,n}$	Thickness
i_{app}	Applied current
j	Ionic flux
a_s	Solid particle surface area
$R_{p,n}^s$	Solid particle radius
A	Surface area of the electrode
D_{eff}^s	Effective solid particle diffusivity
$D_{p,n}^s$	Solid particle diffusivity
D_{eff}^e	Effective electrolyte diffusivity
c_s	Lithium concentration in solid particle
c_e	Lithium-ion concentration in electrolyte
c_s^{max}	Maximum solid particle concentration
c_s^*	Surface concentration
D_e	Electrolyte diffusivity
t_+	Transference number
$\epsilon_{p,s,n}$	Porosity
κ_{eff}^e	Effective electrolyte conductivity
κ_D	Diffusional conductivity
$k_{p,n}$	Reaction rate constant
E_a^k	Reaction constant activation energy
R	Universal gas constant
F	Faraday's constant
α	Transfer coefficient
η	Overpotential
$\rho_{p,n}$	Density
C_p	Specific heat
$\lambda_{Al,p,s,n,Cu}$	Thermal conductivity
T	Temperature
Q_{ohm}	Ohmic generation rate
Q_{rxn}	Reaction generation rate
Q_{rev}	Reversible generation rate
η_n	Overpotential in negative electrode
U_{ref}	Equilibrium potential
R_{film}	Film resistance
R_{SEI}	Initial SEI layer resistance
δ_{film}	Formed film thickness
κ_{SEI}	SEI layer conductivity

⋆ p, s, and n indicate the cathode, separator, and anode.
⋆ Al, and Cu indicate the Al and Cu current collector.

convergence tends to be fast and steady. Conversely, a weakly identifiable parameter has an inconsistent and non-directional effect on optimizing the objective function, and its convergence tends to be slow and even difficult to achieve. In fact, each parameter of the P2D model has a different effect on the voltage and temperature profiles [7], [12]–[15]; thus, those parameters have different identifiabilities when the objective function involves these profiles. As the convergence rates of the parameters depend significantly on their identifiabilities, a suitable search space size should be determined for estimating the parameters more efficiently and accurately. For a strongly identifiable target parameter, a small search space is helpful to avoid inefficient exploration and provide fast convergence. For a weakly identifiable target parameter, a large search space is more appropriate for ensuring that a better solution is found. In HS, the search space size can be

adjusted using the bandwidth. Although it uses the adjusted PAR and bandwidth for a rapid convergence rate, it does not consider the unequal identifiability between the parameters to be estimated. Hence, we develop an HS-based efficient parameter estimation algorithm that employs an adaptive bandwidth according to the identifiability of the parameters.

## C. BANDWIDTH PARAMETERS FOR ADAPTIVE EXPLORATION

Here, the unequal identifiability of the parameters is considered to ensure efficient estimation. Quantitatively, the identifiability of a parameter is obtained from its variability, which is computed either individually or jointly from the distribution of previously estimated parameters. To calculate these variabilities, a memory of candidate parameter sets (PBM) is employed, as shown in Fig. 2, which is a superset of the current HM and stores a given number of the superior candidate parameter sets generated up to the current iteration. Each row and column of PBM represents one harmony and the values of a pitch, or parameter, of the harmonies, respectively. The past best memory size (PBMS) indicates the number of harmonies stored in the PBM. The individual and joint variabilities of each parameter in the PBM are determined from their independent and correlated distributions, respectively. From these variabilities, the proposed AEHS employs two types of bandwidth parameters, which is not the case for existing HS algorithms. These bandwidth parameters obtained from individual and joint variabilities are denoted as $bw_{idv}(itr)$ and $bw_{jnt}(itr)$, respectively.

Individual variabilities of parameters provide a hyper-rectangular region where a sample point, or a $bw_{idv}(itr)$, is selected with uniform probability. Each edge of this hyper-rectangular region has a length proportional to the standard deviation of the distribution of the corresponding parameter, as seen in Fig. 3. Joint variabilities of harmonies in the PBM provide the hyper-ellipsoidal region where a sample point, or $bw_{jnt}(itr)$, is selected with uniform probability. Each semi-axis of the hyper-ellipsoid is proportional to the corresponding eigenvector computed from the joint variabilities of harmonies in the PBM, as seen in Fig. 4. In Fig. 3 and 4, a proportional coefficient is denoted by α.
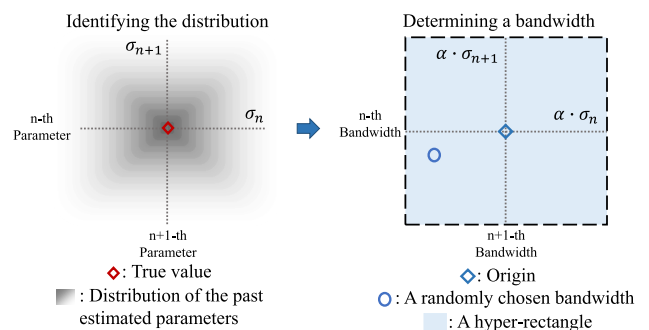
FIGURE 3. Determination of bandwidth parameters, $bw_{idv}(itr)$, according to the individual variability computed from the distributions of past estimated parameters.
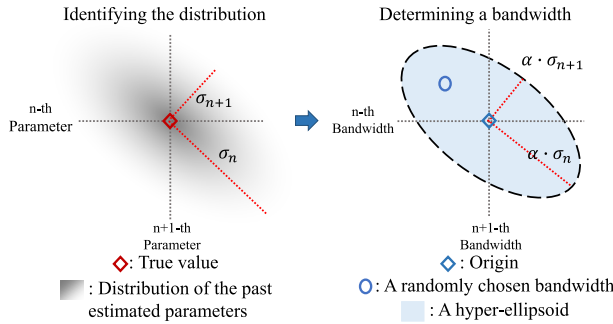
FIGURE 4. Determination of bandwidth parameters, $bw_{jnt}(itr)$, according to the joint variability computed from the distributions of past estimated parameters.

FIGURE 5. Gradually shrinking search space with a decreasing bandwidth parameter that becomes increasingly dependent on the joint variability due to the increase in $P_{choice}(itr)$ and hence makes $bw_{jnt}(itr)$ be selected more than $bw_{idv}(itr)$.

At every iteration, either $bw_{idv}(itr)$ or $bw_{jnt}(itr)$ is employed when generating a new harmony. In the early iteration steps, $bw_{idv}(itr)$ is more frequently adopted as a bandwidth parameter because correlations between the parameters are not clear; hence, it is desirable to not consider them for more effective exploration. As the iteration proceeds, $bw_{jnt}(itr)$ is more frequently selected than $bw_{idv}(itr)$ because the correlations between parameters become clear; hence, it becomes efficient to consider them. The probability for choosing between $bw_{idv}(itr)$ and $bw_{jnt}(itr)$ is given as:

$$P_{choice}(itr) = min\left[\frac{(\epsilon + 1)^{\frac{itr}{\delta \cdot itr_{max}}} - 1}{\epsilon}, 1\right]. \qquad (3)$$

Finally, the bandwidth is obtained as follows:

$$bw(itr) = \begin{cases} bw_{jnt}(itr). \text{ with Prob. } P_{choice}(itr) \\ bw_{idv}(itr). \text{ with Prob. } 1 - P_{choice}(itr) \end{cases} \qquad (4)$$

If the iteration number is lower than $\delta \cdot itr_{max}$, we obtain $P_{choice}(itr) = \frac{1}{\epsilon}((\epsilon + 1)^{\frac{itr}{\delta \cdot itr_{max}}} - 1)$. Otherwise, we obtain $P_{choice}(itr) = 1$. The selecting ratio can be modified by adjusting the positive-value ϵ and $\delta \in (0, 1]$.

As the algorithm progresses, the parameter distribution of the PBM gradually converges to the global optimum. Therefore, the search space for parameter estimation shrinks around the global optimum with the convergence of $bw_{idv}(itr)$ and $bw_{jnt}(itr)$, as seen in Fig. 5. The overall scheme of AEHS is shown in Fig. 6, together with the proposed strategies (in light shading).

IV. RESULTS AND DISCUSSION

A. ALGORITHM IMPLEMENTATION

For the P2D model simulation, LIONSIMBA is employed, which is a set of fully customizable Matlab functions suitable for simulating the dynamic behavior of lithium-ion batteries [22]. The values of the design parameters for AEHS are set as follows : $HMS = 8$, $PBMS = 35$, $HMCR = 0.95$, $PAR_{min} = 0.3$, $PAR_{max} = 0.99$, $itr_{max} = 10000$, $\delta = 0.8$, $\epsilon = 10$, and α is an appropriate function of the iteration number that decreases exponentially from 3 to 2. At each iteration, AEHS generates a new harmony. This new parameter set is entered into the
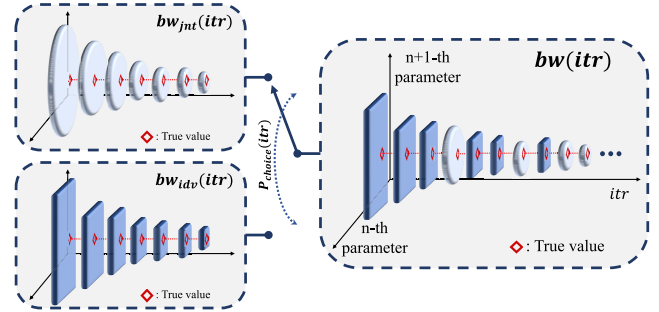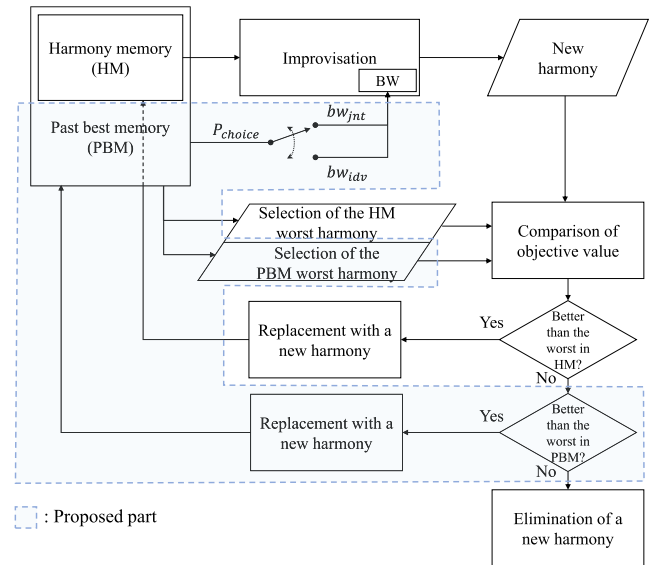
FIGURE 6. Flow chart of the AEHS used in this study.

P2D model simulator, which computes the corresponding voltage and temperature profiles. Then, the objective function value for evaluating a new parameter set is obtained from the simulated profiles (Fig. 7). The objective function used
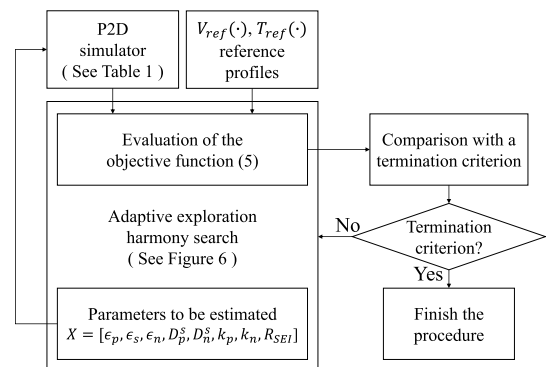
FIGURE 7. Application of AEHS to parameter estimation based on a P2D model.

here is the sum of the squares of the normalized voltage and temperature error, which is given as follows:

$$\sum_{t=1}^{t_f}\left[\left(\frac{V_{ref}(t)-\hat{V}_{sim}(\hat{X},t)}{V_{ref}^{max}}\right)^2+\left(\frac{T_{ref}(t)-\hat{T}_{sim}(\hat{X},t)}{T_{ref}^{max}}\right)^2\right]. \quad (5)$$

where $\hat{X}$ represents the generated parameter set, $V_{ref}(\cdot)$, $\hat{V}_{sim}(\cdot)$, $T_{ref}(\cdot)$, and $\hat{T}_{sim}(\cdot)$ represent the reference and simulation profiles of the terminal voltage and internal temperature, V_{ref}^{max} and T_{ref}^{max} are the maximum, or peak values of the reference terminal voltage and internal temperature profiles, and t_f represents the length of the profiles. This process repeats until the iteration number reaches a predetermined maximum, itr_{max}. During the estimation, the parameter set corresponding to the voltage and temperature profiles most similar to the $V_{ref}(\cdot)$ and $T_{ref}(\cdot)$ is taken as the best parameter set.

B. VALIDATION OF PARAMETER ESTIMATION

In order to validate the parameter estimation performance of the proposed AEHS, a simulation is carried out using three porosities (cathode, separator, anode), two solid particle diffusivities (cathode, anode), two reaction rates (cathode, anode), and SEI layer resistance as unknown parameters to be estimated. The discharging and charging operation of one cycle is set using predetermined conditions: 5C-rate discharge for 200 s with an initial state-of-charge (SOC) of 95%, rest for 100 s, 3C-rate charge with a cut-off voltage of 4.17 V, and charge in constant voltage (CV) mode until a total one-cycle operation time of 500 s.

The bandwidth parameter of the proposed AEHS is determined to achieve the appropriate search space size according to the identifiability of parameters. The magnitudes of the bandwidth parameters for three estimated parameters are shown in Fig. 8. Each trajectory is normalized and smoothed using a 20-point order moving average filter to identify the differences in the trends of the bandwidth parameters. As the anode porosity is strongly identifiable, its bandwidth parameter rapidly converges to zero. This means that the estimation of anode porosity is effective with short duration exploration
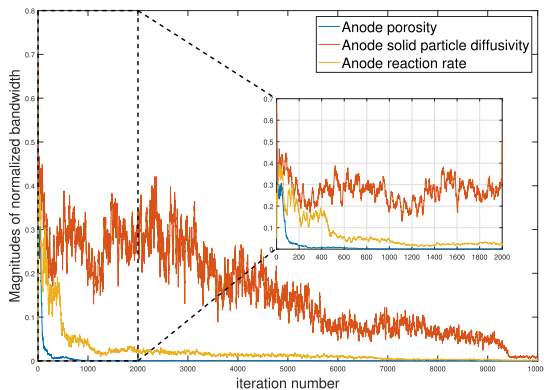
and long duration fine-tuning. On the other hand, the anode solid particle diffusivity has a relatively large bandwidth parameter due to its weak identifiability. This means that the estimation of anode solid particle diffusivity is effective with long duration exploration. In summary, the proposed AEHS provides an efficient search space size in accordance with parameter identifiability.

Five existing metaheuristic algorithms: IHS, SGHS, IGHS, GA, and PSO, were employed to compare the performance of the convergence rate and parameter estimation error. HS based algorithms including the proposed one set the HS parameters such as memory size, HMCR, PAR_{min}, and PAR_{max} identically for fair comparison. For GA, the number of population is set as 25, and the number of particle is set as 2500 for PSO. The objective function values and their corresponding normalized parameter errors are shown in Fig. 9 and 10, respectively. In Fig. 9, all results are obtained by averaging the results simulated five times in the identical condition. We observe that the proposed AEHS has the fastest convergence rate. In terms of the objective function (5), the AEHS has a 0.0073 times lower objective function value than the second best algorithm. As in Fig. 9, all results shown in Fig. 10 are obtained by averaging the results simulated five times in the identical condition. AEHS has the lowest parameter estimation error of 1.20%. The second best algorithm, GA, has a parameter estimation error of 7.98%.
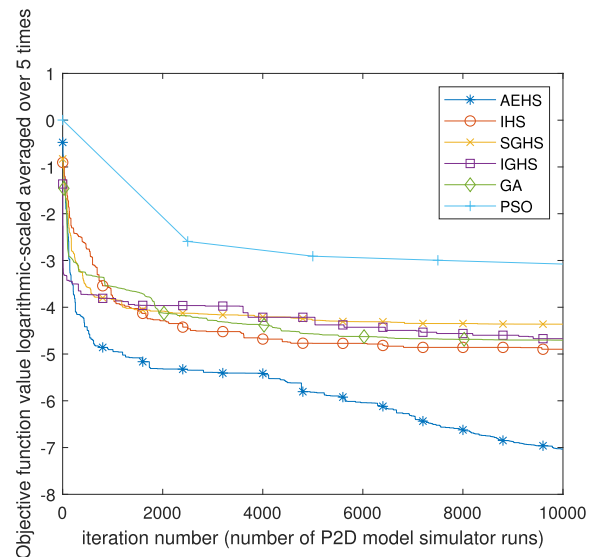

FIGURE 9. Average objective function values against iteration number.

Table 3 summarizes the magnitudes of the parameter estimation errors and the normalized standard deviations of the estimated parameters obtained through five simulations. The normalized standard deviations reveal the reliability of the corresponding estimated values. The proposed AEHS shows small parameter estimation errors with high reliability. The computation time of each algorithm including AEHS is shown in Table 4. Since all algorithms in Table 4 carry out

FIGURE 8. The trajectories of the bandwidths according to the parameter identifiability.

TABLE 3. Estimated parameter values and their normalized standard deviations.

	Porosity $\epsilon_{p,s,n}$ [·]			Solid particle diffusivity $D_{p,n}^s$ [$m^2 s^{-1}$]		Reaction rate $k_{p,n}$ [$m^{2.5} mol^{-0.5} s^{-1}$]		SEI resistance R_{SEI} [Ωm^2]
Reference parameter values								
True values	0.385	0.724	0.485	1.00E-14	3.90E-14	2.33E-11	5.03E-11	1E-3
Magnitudes of parameter estimation errors averaged over five simulations (%)								
IHS	0.16	0.15	0.38	5.54	31.63	3.98	24.98	8.41
IGHS	0.13	0.17	0.24	8.98	33.25	1.96	38.19	13.72
SGHS	0.33	0.20	0.72	9.15	27.57	5.47	35.10	13.95
PSO	0.50	1.64	2.28	15.76	15.50	5.81	19.60	16.85
GA	0.32	0.26	0.68	9.86	20.44	3.41	21.03	7.84
AEHS	**0.02**	**0.02**	**0.03**	**0.16**	**6.33**	**0.23**	**2.01**	**0.81**
Normalized standard deviations of estimated parameters over five simulations								
IHS	0.0019	0.0017	0.0046	0.0653	0.2719	0.0249	0.1295	0.0382
IGHS	0.0015	0.0018	0.0031	0.0221	0.2365	0.0249	0.1110	0.0233
SGHS	0.0048	0.0021	0.0098	0.1221	0.3192	0.0577	0.1607	0.0546
PSO	0.0060	0.0147	0.0181	0.2359	0.2067	0.0630	0.1853	0.1200
GA	0.0044	0.0037	0.0100	0.1271	0.2689	0.0421	0.2139	0.0790
AEHS	**0.0002**	**0.0001**	**0.0005**	**0.0019**	**0.0705**	**0.0038**	**0.0307**	**0.0132**
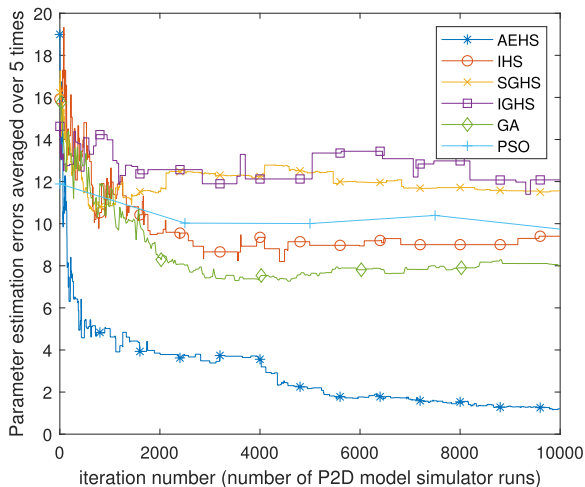
FIGURE 10. Average parameter estimation errors against iteration number.

TABLE 4. Comparison of computation time.

Algorithm	Computation time (hour)
IHS	8.69
IGHS	9.88
SGHS	10.17
PSO	11.70
GA	10.23
AEHS	10.28
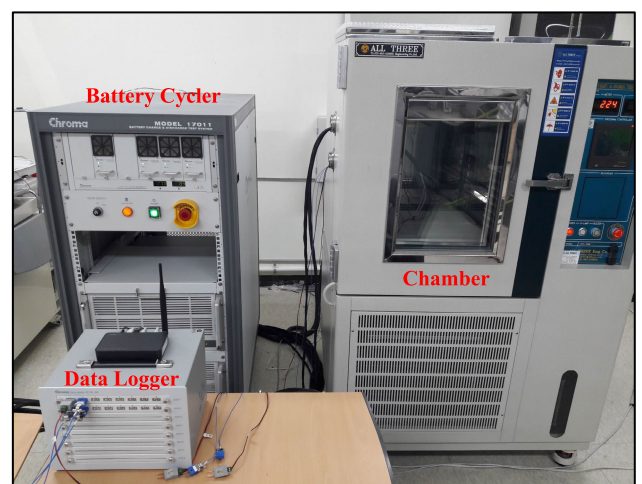
FIGURE 11. A battery testing system with a battery cycler, a data logger, and a chamber.

the time-consuming electrochemical model computation in common, there is no big difference among their computation times.

C. VALIDATION USING REAL MEASURED DATA

To validate the robustness of the proposed algorithm, the additional experiments are conducted with two batteries having totally different aging states. The parameter information of the battery adopted for the experiment is partially given; therefore, more parameters are estimated to determine the dynamics of the reference profile than in the simulation validation. As well as the eight predetermined target parameters specified in (1), two solid particle surface areas

(cathode, anode), one current collector conductivity (anode), two solid particle conductivity (cathode, anode), one electrolyte diffusivity, two solid particle radii (cathode, anode),

and the initial state of charge (SOC) are additionally estimated. The objective function for this estimation only considers the square normalized voltage error, which has the form of (5) without the temperature related term. The employed current in the experiments is basically GITT (Galvanostatic Intermittent Titration Technique) profiles composed of 1C-rate discharge for 5% SOC decrease and 30 minutes rest. It is observed that the mean errors between the measured profile and the one simulated from the estimated parameters reach 1.6 mV for battery #1, and 1.7mV for battery #2.

In Fig. 12 and 13, first 5,000 seconds of the measured data are used for estimating the parameters with the proposed algorithm, AEHS, and then, total 8,000 seconds of the measured data are compared with the simulated profiles to validate the estimated parameters. The dashed line represents the simulated voltage profile obtained from the estimated parameters and the solid line designates the measured voltage profile. The mean voltage errors between the two profiles are
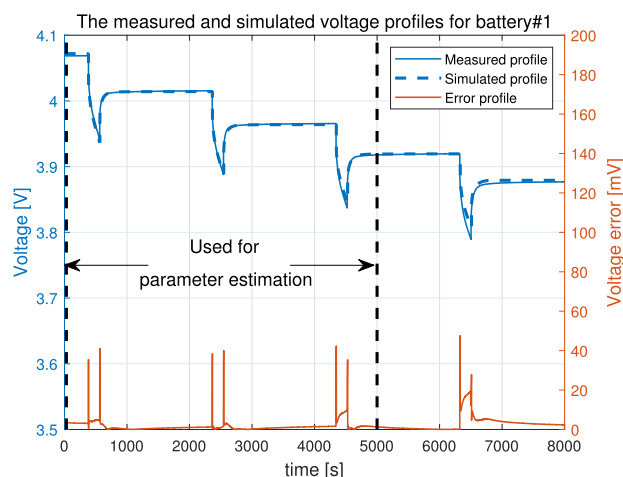
FIGURE 12. Comparison between the measured and simulated voltage profiles of battery#1.
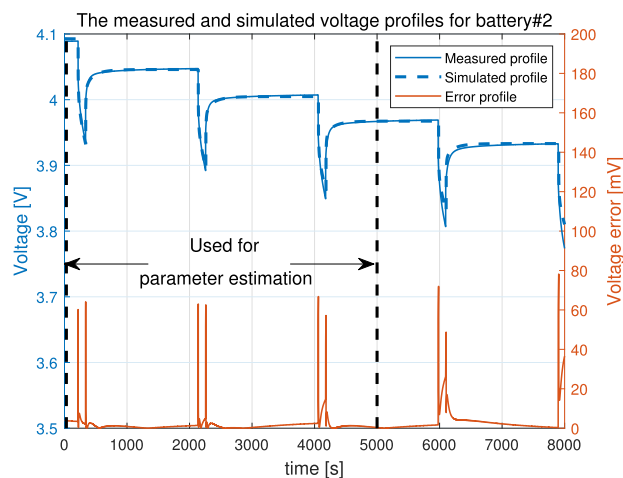
FIGURE 13. Comparison between the measured and simulated voltage profiles of battery#2.

only 2.1mV for battery #1 and 2.5mV for battery#2. It is observed that the simulated profiles accurately follow the measured ones even for the different operation conditions from those for parameter estimation. In this sense, it could be said that the proposed method works well for various types of batteries.

V. CONCLUSION

This study proposed a new adaptive exploration strategy based on HS, called AEHS, that considers the unequal identifiabilities among the parameters of an electrochemical lithium-ion battery model. For more efficient estimation, a parameter with low identifiability is estimated by exploring a wide search space for a longer period of time compared with a parameter with high identifiability. The degree of identifiability is predicted from the individual and joint variabilities computed from the distributions of previously estimated parameters, and reflected by the bandwidth parameters of the proposed AEHS. A numerical validation with eight parameters related to the aging process of a lithiumion battery showed that the proposed AEHS reduced inefficient exploration to ensure rapid convergence and enabled exploration that can achieve global optimality. The optimized objective function value of AEHS amounted to approximately one hundredth of the value of the second best algorithm analyzed in this study. This resulted in the smallest parameter estimation error of 1.20%, whereas the second best algorithm achieved a value of 7.98%. Moreover, the voltage profiles simulated using 17 parameters estimated from real data were very close to the real measured profiles, with the average differences between them only 2.1mV and 2.5mV for each battery, respectively.

In conclusion, we suggest that our proposed AEHS scheme is a good choice for recovering the internal physical parameters of a lithium-ion battery to ensure more efficient and safe management of the battery. We believe that the proposed AEHS has many other applications for the monitoring, management, and diagnosis of lithium-ion batteries in terms of extending their lifespan and preventing accidents.

REFERENCES

[1] M. Broussely, P. Biensan, F. Bonhomme, P. Blanchard, S. Herreyre, K. Nechev, and R. J. Staniewicz, "Main aging mechanisms in Li ion batteries," *J. Power Sources*, vol. 146, nos. 1–2, pp. 90–96, 2005.

[2] K. Uddin, S. Perera, W. Widanage, L. Somerville, and J. Marco, "Characterising lithium-ion battery degradation through the identification and tracking of electrochemical battery model parameters," *Batteries*, vol. 2, no. 2, p. 13, 2016.

[3] P. Verma, P. Maire, and P. Novák, "A review of the features and analyses of the solid electrolyte interphase in Li-ion batteries," *Electrochimica Acta*, vol. 55, no. 22, pp. 6332–6341, 2010.

[4] V. Ramadesigan, K. Chen, N. A. Burns, V. Boovaragavan, R. D. Braatz, and V. R. Subramanian, "Parameter estimation and capacity fade analysis of lithium-ion batteries using reformulated models," *J. Electrochem. Soc.*, vol. 158, no. 9, pp. A1048–A1054, 2011.

[5] Q. Li, W. Chen, Y. Wang, S. Liu, and J. Jia, "Parameter identification for PEM fuel-cell mechanism model based on effective informed adaptive particle swarm optimization," *IEEE Trans. Ind. Electron.*, vol. 58, no. 6, pp. 2410–2419, Jun. 2011.

[6] J. Li, L. Zou, F. Tian, X. Dong, Z. Zou, and H. Yang, "Parameter identification of lithium-ion batteries model to predict discharge behaviors using heuristic algorithm," *J. Electrochem. Soc.*, vol. 163, no. 8, pp. A1646–A1652, 2016.

[7] J. C. Forman, S. J. Moura, J. L. Stein, and H. K. Fathy, "Genetic identification and Fisher identifiability analysis of the Doyle–Fuller–Newman model from experimental cycling of a LiFePO₄ cell," *J. Power Sources*, vol. 210, pp. 263–275, Jul. 2012.

[8] L. Zhang, L. Wang, G. Hinds, C. Lyu, J. Zheng, and J. Li, "Multi-objective optimization of lithium-ion battery model using genetic algorithm approach," *J. Power Sources*, vol. 270, pp. 367–378, Dec. 2014.

[9] M. A. Rahman, S. Anwar, and A. Izadian, "Electrochemical model parameter identification of a lithium-ion battery using particle swarm optimization method," *J. Power Sources*, vol. 307, pp. 86–97, Mar. 2016.

[10] A. Askarzadeh and A. Rezazadeh, "An innovative global harmony search algorithm for parameter identification of a PEM fuel cell model," *IEEE Trans. Ind. Electron.*, vol. 59, no. 9, pp. 3473–3480, Sep. 2012.

[11] A. Maleki and F. Pourfayaz, "Sizing of stand-alone photo-voltaic/wind/diesel system with battery and fuel cell storage devices by harmony search algorithm," *J. Energy Storage*, vol. 2, pp. 30–42, Aug. 2015.

[12] A. P. Schmidt, M. Bitzer, A. W. Imre, and L. Guzzella, "Experiment-driven electrochemical modeling and systematic parameterization for a lithium-ion battery cell," *J. Power Sources*, vol. 195, no. 15, pp. 5071–5080, 2010.

[13] Z. Deng, H. Deng, L. Yang, Y. Cai, and X. Zhao, "Implementation of reduced-order physics-based model and multi-parameters identification strategy for lithium-ion battery," *Energy*, vol. 138, pp. 509–519, Nov. 2017.

[14] C. Edouard, M. Petit, C. Forgez, J. Bernard, and R. Revel, "Parameter sensitivity analysis of a simplified electrochemical and thermal model for Li-ion batteries aging," *J. Power Sources*, vol. 325, pp. 482–494, Sep. 2016.

[15] L. Zhang, C. Lyu, G. Hinds, L. Wang, W. Luo, J. Zheng, and K. Ma, "Parameter sensitivity analysis of cylindrical LiFePO₄ battery performance using multi-physics modeling," *J. Electrochem. Soc.*, vol. 161, no. 5, pp. A762–A776, 2014.

[16] Z. W. Geem, J. H. Kim, and G. V. Loganathan, "A new heuristic optimization algorithm: Harmony search," *J. Simul.*, vol. 76, no. 2, pp. 60–68, Feb. 2001.

[17] M. G. H. Omran and M. Mahdavi, "Global-best harmony search," *Appl. Math. Comput.*, vol. 198, no. 2, pp. 643–656, 2008.

[18] C. Peraza, F. Valdez, and O. Castillo, "A harmony search algorithm comparison with genetic algorithms," in *Fuzzy Logic Augmentation of Nature-Inspired Optimization Metaheuristics*. Cham, Switzerland: Springer, 2015, pp. 105–123.

[19] Y.-H. Kim, Y. Yoon, and Z. W. Geem, "A comparison study of harmony search and genetic algorithm for the max-cut problem," *Swarm Evol. Comput.*, vol. 44, no. 2, pp. 130–135, Feb. 2019.

[20] M. Mahdavi, M. Fesanghary, and E. Damangir, "An improved harmony search algorithm for solving optimization problems," *Appl. Math. Comput.*, vol. 188, no. 2, pp. 1567–1579, May 2007.

[21] W. G. Gray and P. C. Y. Lee, "On the theorems for local volume averaging of multiphase systems," *Int. J. Multiphase Flow*, vol. 3, no. 4, pp. 333–340, 1977.

[22] M. Torchio, L. Magni, R. B. Gopaluni, R. D. Braatz, and D. M. Raimondo, "LIONSIMBA: A MATLAB framework based on a finite volume model suitable for Li-ion battery design, simulation, and control," *J. Electrochem. Soc.*, vol. 163, no. 7, pp. A1192–A1205, 2016.

[23] S. Santhanagopalan, Q. Guo, P. Ramadass, and R. E. White, "Review of models for predicting the cycling performance of lithium ion batteries," *J. Power Sources*, vol. 156, no. 2, pp. 620–628, 2006.

[24] P. Ramadass, B. Haran, P. M. Gomadam, R. White, and B. N. Popov, "Development of first principles capacity fade model for Li-ion cells," *J. Electrochem. Soc.*, vol. 151, no. 2, pp. A196–A203, 2004.

[25] G. Sikha, B. N. Popov, and R. E. White, "Effect of porosity on the capacity fade of a lithium-ion battery theory," *J. Electrochem. Soc.*, vol. 151, no. 7, pp. A1104–A1114, 2004.

[26] A. P. Schmidt, M. Bitzer, Á. W. Imre, and L. Guzzella, "Model-based distinction and quantification of capacity loss and rate capability fade in Li-ion batteries," *J. Power Sources*, vol. 195, no. 22, pp. 7634–7638, 2010.

[27] E. Prada, D. Di Domenico, Y. Creff, J. Bernard, V. Sauvant-Moynot, and F. Huet, "A simplified electrochemical and thermal aging model of LiFePO₄-graphite li-ion batteries: Power and capacity fade simulations," *J. Electrochem. Soc.*, vol. 160, no. 4, pp. A616–A628, 2013.

[28] Q.-K. Pan, P. N. Suganthan, M. F. Tasgetiren, and J. J. Liang, "A self-adaptive global best harmony search algorithm for continuous optimization problems," *Appl. Math. Comput.*, vol. 216, no. 3, pp. 830–848, 2010.

[29] Z. W. Geem and Y. Yoon, "Harmony search optimization of renewable energy charging with energy storage system," *Int. J. Elect. Power Energy Syst.*, vol. 86, pp. 120–126, Mar. 2017.

HUIYONG CHUN was born in Seoul, South Korea, in 1994. He received the B.S. degree in electrical engineering from the Pohang University of Science and Technology (POSTECH), Pohang, South Korea, in 2017, where he is currently pursuing the Ph.D. degree with the Department of Creative IT Engineering. His research interests include lithium-ion battery state and parameter estimation, battery management systems, and machine learning applications in lithium-ion battery.
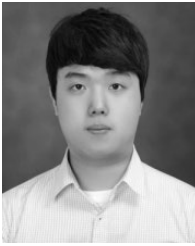
MINHO KIM received the B.S. degree in mechanical engineering from Korea University, Seoul, South Korea, in 2015. He is currently pursuing the Ph.D. degree with the Department of Creative IT Engineering, Pohang University of Science and Technology (POSTECH), Pohang, South Korea. His main research interests include energy storage systems and machine learning technology

JUNGSOO KIM was born in Seoul, South Korea. He received the B.S. degree in mechanical engineering from Korea University, Seoul, South Korea, in 2013. He is currently pursuing the Ph.D. degree (M.S–Ph.D. integrated program) with the Department of Creative IT Engineering (CiTE), Pohang University of Science and Technology (POSTECH), Pohang, South Korea. His research interests include li-ion battery state estimation, li-ion battery parameter identification, battery management systems, and their applications to electric vehicles and smart grids.

KWANGRAE KIM received the B.S. degree in electrical engineering from Konkuk University, Seoul, South Korea, in 2015, and the M.S. degree in electrical engineering from the Pohang University of Science and Technology (POSTECH), Pohang, South Korea, in 2018, where he is currently pursuing the Ph.D. degree in electrical engineering. His research interests include lithium-ion battery state estimation, battery management systems, and optimization applications in battery field.

JUNGWOOK YU received the B.S. degree in information management and technology from Syracuse University, NY, USA, in 2012. He is currently pursuing the Ph.D. degree with the Department of Creative IT Engineering, Pohang University of Science and Technology (POSTECH), Pohang, South Korea. His research interests include battery management systems, parameter estimation, and neural networks.

TAEGYUN KIM received the B.S. and M.S. degrees in electrical engineering from the Pohang University of Science and Technology (POSTECH), Pohang, South Korea, in 2013 and 2016, respectively, where he is currently pursuing the Ph.D. degree in electrical engineering. His main research interest includes control and management of Li-ion batteries.

SOOHEE HAN received the B.S., M.S. degrees in electrical engineering, and Ph.D. degree in computer science from Seoul National University (SNU), Seoul, South Korea, in 1998, 2000, and 2003, respectively, where he was a Researcher with the Engineering Research Center for Advanced Control and Instrumentation, from 2003 to 2007. In 2008, he was a Senior Researcher with the Robotics S/W Research Center. From 2009 to 2014, he was with the Department of Electrical Engineering, Konkuk University, Seoul. Since 2014, he has been with the Department of Creative IT Engineering, Pohang University of Science and Technology, Pohang, South Korea. His research interests include computer aided control system designs, distributed control systems, time delay systems, and stochastic signal processing.

● ● ●